Progress In Electromagnetics Research B, Vol. 30, 71–82, 2011

APPLICATION OF SUPER-SVA TO STEPPED-CHIRP RADAR IMAGING WITH FREQUENCY BAND GAPS BETWEEN SUBCHIRPS

W. Zhai †

Graduate University of the Chinese Academy of Sciences
Beijing 100039, China

Y. Zhang ‡

The Key Laboratory of Microwave Remote Sensing, Chinese Academy of Sciences
Beijing, China

Abstract—It is well-known that the stepped-frequency chirp signal (SFCS) technique is one of the very effective approaches for achieving high range resolution in radar [1–5]. The SFCS is a train of subchirp pulses with up-stepped or down-stepped carrier frequencies. However, there exists a rang-Doppler coupling problem (RDCP) when applying this signal to practical radar system because longer time is needed for transmitting a complete burst compared with that needed for transmitting just a single chirp. In radar system design, if carrier frequency step (Δf) can be larger than the bandwidth of subchirp (B_m), it will be very helpful for using less number of subchirps to obtain high resolution and at the same time reduce the influence of RDCP on imaging quality. However, the spectrum of transmitted signal will not be continuous but with band gaps existing when $\Delta f > B_m$, and it will lead to high grating lobes in range profile. In this paper, the Super-SVA technique is applied to solve the grating lobe problem arisen from band gaps in SFCS. Simulation and experiment results for moving train imaging are presented to show that the algorithm works very well.

Received 28 March 2011, Accepted 26 April 2011, Scheduled 29 April 2011
Corresponding author: Wenshuai Zhai (zhaiwenshuai@nmrs.ac.cn).
† Also with The Key Laboratory of Microwave Remote Sensing, Chinese Academy of Sciences, and Center for Space Science and Applied Research, Chinese Academy of Sciences, Beijing 100190, China.
‡ Also with Center for Space Science and Applied Research, Chinese Academy of Sciences, Beijing 100190, China.

1. INTRODUCTION

In SAR imaging, range resolution is inversely proportional to the transmitted signal bandwidth, but the hardware technology and also the cost issues make the system bandwidth limited. To meet the requirements of higher resolution, stepped frequency technique has become an alternative method for radar systems. Stepped frequency chirp signal (SFCS), as an important signal form of SAR imaging, has been used to achieve high resolution with low instantaneous bandwidth and low sampling rate, and has been paid more and more attention [1–6]. By transmitting a train of narrow-bandwidth chirp pulses carried on stepped frequencies, the corresponding echoes are then received and synthesized into a much wider band signal so as to achieve high range resolution. However, the number of subpulses that can be coherently combined in SFCS is usually limited in practical radar system because the motion compensation issue becomes much more complicated when the number increases. But reducing the subpulse number usually means reducing the synthesized bandwidth. If choosing the frequency step (Δf) to be larger than the bandwidth of subchirp (B_m), we can use less number of subchirps to cover the same wide spectrum as in the case of $\Delta f \leqslant B_m$. However, when $\Delta f > B_m$, the frequency band of adjacent subpulses will not be overlapped, that will finally result in the grating lobes in range profile. In this paper, it is shown that Super Spatially Variant Apodization (Super-SVA) technique can be used to solve the problem.

Super-SVA is a robust super resolution technique developed by Stankwitz and Kosek [7]. It can be used to extrapolate the signal spectrum without requiring a priori knowledge about the scene. Xu and Narayanan successfully used it to enhance the resolution of SAR/ISAR with real data [8]. Stankwitz and Kosek also proposed that it can be used to interpolate gapped SAR data when certain received data are lost due to hardware error or interfering sources [9]. Zhuang et al. applied it to sparse aperture radar imaging to get full aperture data [10]. In this paper we propose to apply Super-SVA to processing SFCS with bandwidth gaps. Simulations in our previous papers [11, 12] have verified that it can be adopted to fill the band gaps between subpulses and thus depress grating lobes efficiently. This paper focuses on the experiment with a Ku-band stepped frequency radar experimental system. In the experiment B_m is 60 MHz and Δf is 100 MHz. That is to say, there is 40 MHz band gap between adjacent subpulses in frequency domain. Via 20 steps, the synthesized bandwidth can reach up to 2 GHz and the image resolution is 0.075 m but grating lobes are very high. By using Super-SVA, correct image

without grating lobes is obtained. Experiment results show good performance of the algorithm that can accomplish the above purpose.

2. SIGNAL MODEL AND SFCS SYNTHETIC PROCESSING

SFCS is a burst of narrow-bandwidth subpulses carried on stepped frequency, which can be described as

$$p_n(t) = \text{rect}\left(\frac{t}{T_p}\right) \exp\left[j2\pi\left(f_n t + \frac{1}{2}kt^2\right)\right] \tag{1}$$

where k and T_p are the FM slope and the pulse width of sub-chirps, respectively. $f_n = f_1 + (n-1)\Delta f$, f_1 is the carrier frequency of the first sub-chirp. Δf is frequency step. $n = 1, 2, \ldots, N$ denotes the number of steps.

The subaperture processing method of SFCS is as follows [13, 14].

(a) to perform match filtering on each sub-pulse after receiving the echo signal.

(b) to shift the nth subpulse frequency by $(n-1)\Delta f$.

(c) to coherently combine all the subpulses in frequency domain.

(d) to perform inverse Fourier transform on the synthesized signal to obtain high resolution range profile.

This method is simple and easy to combine with Super-SVA.

3. THE PRINCIPLE OF SUPER-SVA

Super-SVA is a super resolution technique based on SVA. SVA is an image domain algorithm which can effectively eliminate sidelobes while not broadening the mainlobe [15]. The property of SVA is achieved through the selection of a particular windowing function for each pixel of SAR image. It is based on cosine-on-pedestal frequency domain weighting function:

$$W(n) = 1 + 2\alpha\cos(2\pi n/N), \quad 0 \le \alpha \le 0.5 \tag{2}$$

By taking the discrete Fourier transform, we can get the Nyquist-sampled impulse response (IPR):

$$w(m) = \alpha\delta(m-1) + \delta(m) + \alpha\delta(m+1) \tag{3}$$

So the SVA-filtered image samples will be

$$g'(m) = \alpha(m)g(m-1) + g(m) + \alpha(m)g(m+1) \tag{4}$$

where $g(m)$ are the samples of either the real or the imaginary component of image.

The task of SVA is to find appropriate $\alpha(m)$ to minimize $|g'(m)|^2$ subject to the constraints: $0 \leq \alpha(m) \leq 0.5$. Because $g'(m)$ is a linear function of α, we can calculate the values of $g'(m)$ at $\alpha = 0$ and $\alpha = 0.5$. If the two values have opposite sign, $g'(m) = 0$. Otherwise, select the smaller magnitude of the two values as $g'(m)$.

Super-SVA is developed based on SVA. It can be used to extrapolate signal spectrum in a simple, straightforward and iterative manner by repeatedly using SVA. After first performing FFT on the original data, SVA is applied to the resultant image to remove the side lobes. Then the inverse FFT is performed. Since SVA is a nonlinear operation, the image is no longer band-limited. The next step in the deconvolution process is to apply an inverse amplitude weight to the frequency domain data. The inverse weight function is the inverse Fourier transformation of a SINC function's mainlobe. The weighted signal must be truncated to keep the total extrapolation less than 60% of the original signal so as to avoid singularities in the inverse function. After weighting and truncating, the original signal is used to replace the central portion of the extrapolated signal. The above extrapolation procedure can be repeated several times to get much larger bandwidth. The details of the algorithm can be referred to [7, 8].

4. APPLY SUPER-SVA TO THE PROCESSING OF SFCS WITH BAND GAPS

In SFCS, when $\Delta f > B_m$, as shown in Figure 1, there are no observation data within $(\Delta f - B_m)$ gap between adjacent subpulses'

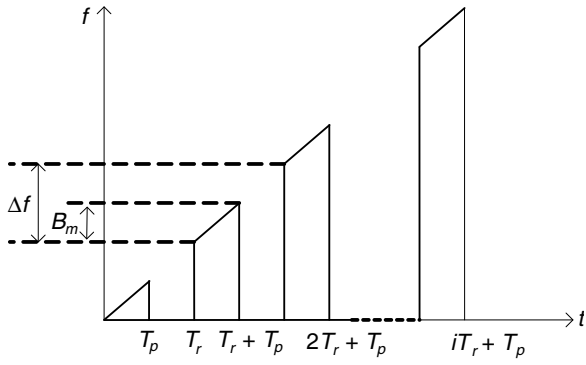

Figure 1. The frequency of SFCS varies with time.

band and the combined spectrum is not continuous. Since Super-SVA is very good for extrapolating data, we shall use it to fill the gaps. In this way we can break the restriction in SFCS design that Δf must be less than B_m and achieve higher resolution by less subpulses.

The transmitted signal is expressed as (1) and the echo signal can be written as (2).

$$s_n(t) = \int_{\tau_1}^{\tau_2} g_n(\tau) p_n(t-\tau) d\tau = g_n(t) * p_n(t) \tag{5}$$

where $\tau = 2r/c$ is the time delay, $r \in [r_1, r_2]$ is the range of the target, $\tau_1 = 2r_1/c$, $\tau_2 = 2r_2/c$, $g_n(\tau)$ is the scattering coefficient of the target corresponding to each subchirp.

The flow chart of the proposed algorithm is presented in Figure 2 and shall be illustrated in the following.

Match filtering is first performed in frequency domain on the echo data

$$G_n(\omega) = S_n(\omega) \cdot P_n^*(\omega) \tag{6}$$

where $S_n(\omega)$ and $P_n(\omega)$ are the Fourier transforms of $s_n(t)$ and $p_n(t)$, respectively. And $*$ represents complex conjugate.

Then Super-SVA is performed on the matched filtered data to estimate the unknown data until the band of each subpulse is larger than Δf.

$$G_n'(\omega) = \text{SuperSVA}\{G_n(\omega)\} \tag{7}$$

Before coherently synthesizing all the subpulse data, the spectrum should be frequency shifted:

$$F_n(\omega) = G_n'(\omega - (n-1)\Delta\omega) \tag{8}$$

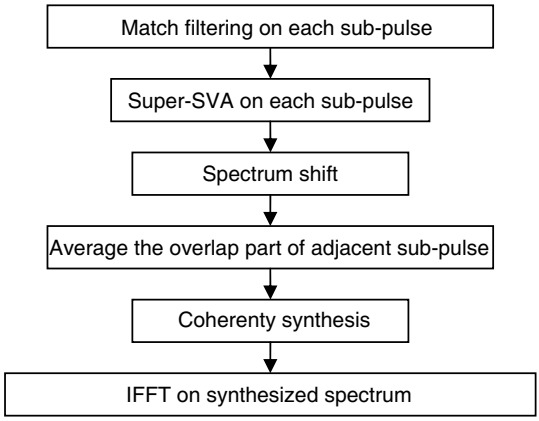

Figure 2. The flow chart of SFCS processing.

where $\Delta\omega = 2\pi\Delta f$. Via spectrum shift, the adjacent subpulses band may overlap with each other. The overlapped parts can be averaged or we can select one half of the former subpulse and another half of the latter one.

$$F'_n(\omega) = \text{rect}\left(\frac{\omega - (n-1)\Delta\omega}{\Delta\omega}\right) F_n(\omega) \tag{9}$$

The next step is to coherently combine all the subpulses:

$$F(\omega) = \sum_{n=1}^{N} F'_n(\omega) \tag{10}$$

Up to now the synthesized spectrum without gaps is obtained. And through IFFT we can finally get high resolution image without grating lobes.

$$f(r) = \text{IFFT}\{F(\omega)\} \tag{11}$$

Further more, the algorithm is also applicable when some subpulses of the whole burst are missing due to system error or some data must be discarded because of being corrupted by interfering sources. In these cases, the missing data can be extrapolated based on the available data to recover the full spectrum.

5. EXPERIMENT AND RESULTS

Our experimental system is a Ku-band radar which uses SFCS. The radar hardware mainly consists of a wideband frequency synthesizer with high-speed switchers, a time sequence controller, a power amplifier, two antennas (one used for transmitting and one used for receiving), a receiver and a data recording device. Table 1 lists the major specifications of the system related to signal processing.

Table 1. Some specifications of the radar system.

Carrier Frequency	13–15 GHz
Frequency Step	100 MHz
Subpulse Bandwidth	60 MHz
Subpulse Width	6 μs
Subpulse Numbers	20
Subpulse PRI	8 μs
PRF	250 Hz
A/D sampling rate	200 Msps

When the number of subpulse N is 20 and the frequency step Δf is 100 MHz, the final range resolution ΔR after synthesizing all of the subpulses can be easily calculated as

$$\Delta R = \frac{1}{N \cdot \Delta f} \cdot \frac{c}{2} = 0.075\,\mathrm{m} \tag{12}$$

Now let's examine the point target response of the system. Figure 3 shows the results obtained without applying Super-SVA. In Figure 3(a), the synthesized bandwidth reaches 2 GHz with 19 gaps of 40 MHz. The discontinuous spectrum will produce high grating lobes in range profile. The larger the gap, the higher the grating lobe will be. These grating lobes will locate at

$$R_{\mathrm{lobes}} = \frac{i}{\Delta f} \cdot \frac{c}{2} = i \times 1.5\,\mathrm{m} \quad i = \pm 1, \pm 2, \ldots \tag{13}$$

From the compression result as shown in Figure 3(b), one can see that the resolution matches to the theoretical value very well and the grating lobes appear exactly at the positions predicted by (13). The highest grating lobe is about -6.5 dB, which is not acceptable. It means that noticeable artifacts might appear in radar image and weak target might be overlapped.

In the following, we shall iteratively perform Super-SVA on each subpulse. In each iteration step, the bandwidth of each subpulses are extrapolated to 130% of the last result. So the extended bandwidth of each subpulse will be larger than 100 MHz after two iterations. Figure 4(a) shows the synthesized spectrum after applying Super-SVA, from which one can see that the gaps existing in Figure 3(a) are all

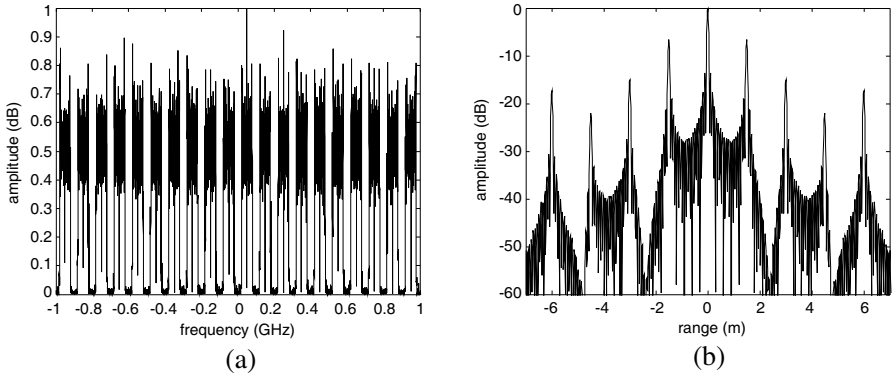

Figure 3. Results without using Super-SVA. (a) Synthesized spectrum. (b) Point target response.

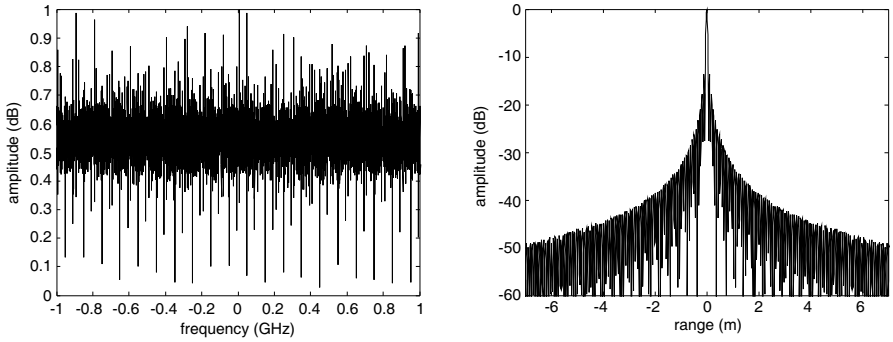

Figure 4. Results with the proposed algorithm described in Section 4. (a) Synthesized spectrum. (b) Point target response.

Figure 5. Imaging target: moving train.

filled. Figure 4(b) shows the correct point target response with grating lobes eliminated as expected.

Figure 5 is a photo of the moving train which is taken as the observation target in our experiment. It is the train of No. 13 light railway line in Beijing. The train has six compartments, each compartment is 19.2 m long and the total length of the train is about 118 m. Figures 6(a) and (b) are the obtained images after both range and azimuth compressions completed. In Figure 6(a) the configuration of the train is indicated very clearly. Six compartments as well as the connections between them are very well imaged. However there exist serious grating lobes, which could be taken as the ghost targets on both sides of the true target location. The first grating lobe pair locates 1.5 m away from the imaged target on both sides, which agrees to the theoretical value. In our experiment, the train occupies only several range bins in the image, so we can easily make a distinction between the mainlobe and the grating lobes. However, in application of large area imaging, high grating lobes would seriously blur the image and degrade the performance of target identification.

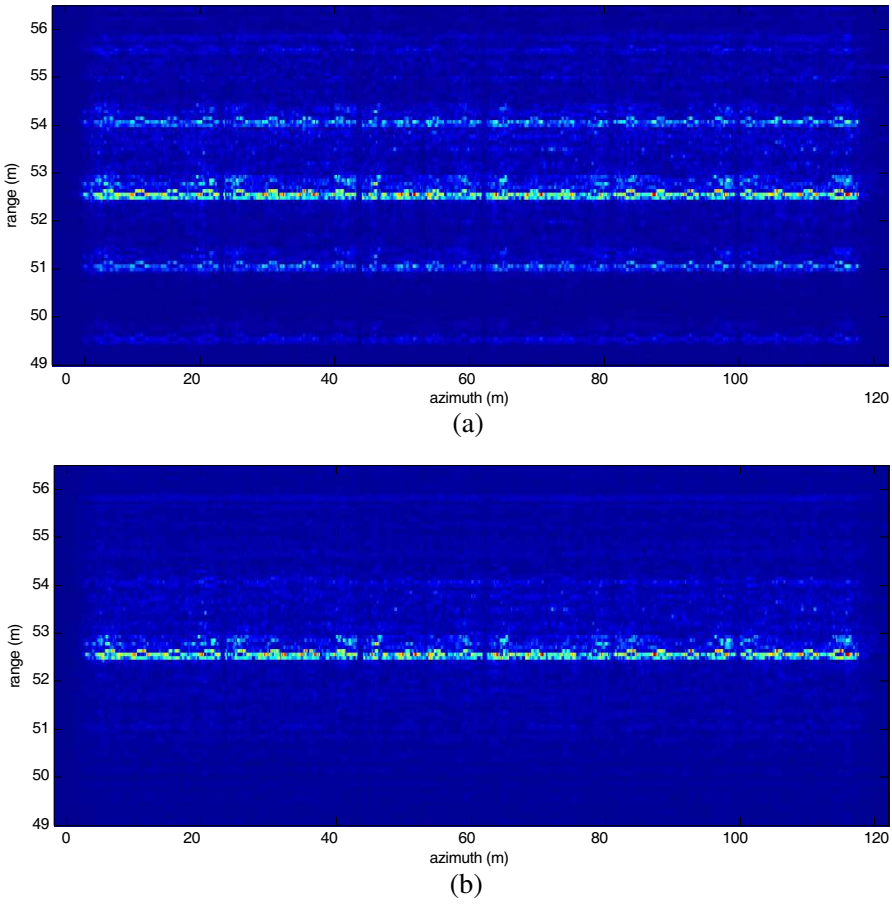

Figure 6. Radar images obtained with and without Super-SVA used. (a) Image without Super-SVA. (b) Image with Super-SVA.

Figure 6(b) is the obtained image with Super-SVA used in signal processing. By comparing Figures 6(b) and 6(a), one can see that the details of the train completely remained while the grating lobes are depressed, i.e., the correct image is recovered. Benefiting from the achieved high resolution, typical scattering points on the train can be distinguished, such as the doors, the windows, and the ventilators of air-conditioners, which are on the top of both ends of each compartment. The length of each compartment in the image can be figured out, which is in good accordance with the real measurement.

Figure 7 presents two range profiles drawn from Figures 6(a) and 6(b), respectively. By comparing these two profiles, one can

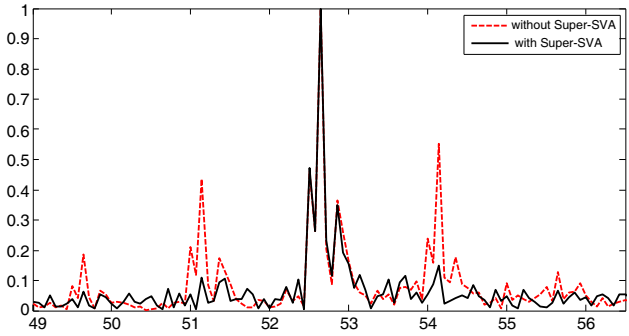

Figure 7. The comparison of range profiles with and without Super-SVA used.

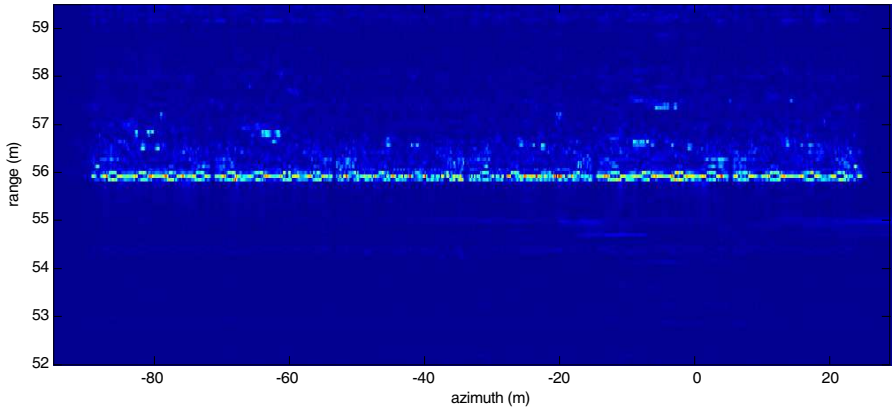

Figure 8. Image with full band.

clearly see that after applying Super-SVA, the grating lobes are very well controlled without losing the resolution. The highest grating lobe decreased more than 10 dB while the main lobe keeps unchanged.

Figure 8 shows the result of another experiment with subpulse bandwidth of 120 MHz used and the other parameters are the same with the previous experiment. Comparing Figure 6(b) with Figure 8, it is shown that by using the proposed algorithm we can obtain the similar image as that obtained from full band, except a little more background noise. Due to the different viewing angles in the two experiments, the ventilators of the train in Figure 8 are not as clear as those in Figure 6 while the doors and windows are much more visible. It's very interesting to note that in the latter experiment, a railway lamp just locates in the boresight of the antenna beams, which can be

found in the right photo of Figure 5. The strong multiple scatterings between the lamp and the smooth top surface of the compartment lead to the uniform clutters in the imaged area above the train, as shown in Figure 8.

6. CONCLUSION

In high resolution radar which uses SFCS, when the frequency step is larger than the bandwidth of subchirp, there will be band gaps in the synthesized spectrum, and ghost targets will definitely exist in the radar image due to the high range grating lobes. It is demonstrated in this paper that by using Super-SVA to extrapolate the bandwidth of each sub-pulse, we can get full spectrum without any gaps. The gap-filled data then can be processed to get image without grating lobes. With this algorithm, we can keep resolution unchanged while reducing the number of sub-pulses, which is beneficial for reducing the influence of rang-Doppler coupling effect on the quality of the synthesized image. The results of real target imaging experiment validated the proposed algorithm.

REFERENCES

1. Levanon, N. and E. Mozeson, *Radar Signals*, Chapter 7, John Wiley & Sons, 2003.
2. Levanon, N., "Stepped-frequency pulse-train radar signal," *IEE Proceedings Radar, Sonar and Navigation*, Vol. 149, No. 6, 297–309, 2002.
3. Zhang, Q., T. S. Yeo, and G. Du, "ISAR imaging in strong ground clutter by using a new stepped-frequency signal format," *IEEE Trans. Geosci. Remote Sensing*, Vol. 41, No. 5, 948–9521, 2003.
4. Gladkova, I. and D. Chebanov, "Suppression of grating lobes in stepped-frequency train," *Proceedings of IEEE International Radar Conference*, 371–376, Arlington, VA, USA, May 2005.
5. Doerry, A. W., "SAR processing with stepped chirps and phased array antennas," *SANDIA Report*, 2006–5855, 2006.
6. Zhai, W., X. Zhang, and Y. Zhang, "Signal processing and resolution analysis of Ka-band stepped-frequency radar in moving target imaging experiment," *Global Symposium on Millimeter Waves 2010 (GSMM 2010)*, 83–86, Incheon, Apr. 14–16, 2010.
7. Stankwitz, H. C. and M. R. Kosek, "Super-resolution for SAR/ISAR RCS measurement using spatially variant apodization," *Proceedings of Antenna Measurement Techniques Associ-*

ation (AMTA) 17th Annual Meeting and Symposium, 251–256, Williamsburg, VA, Nov. 13–17, 1995.

8. Xu, X. and R. M. Narayanan, "Enhanced resolution in SAR/ISAR imaging using iterative sidelobe apodization," *IEEE Transactions on Image Processing*, Vol. 14, No. 4, 537–547, Apr. 2005.
9. Stankwitz, H. C. and M. R. Kosek, "Sparse aperture fill for SAR using Super-SVA," *Proceedings of the 1996 IEEE National Radar Conference*, 70–75, Ann Arbor, May 13–16, 1996.
10. Zhuang, L., X. Liu, and Z. Zhou, "Enhanced resolution for sparse aperture radar imaging using Super-SVA," *Proceedings of Asia-Pacific Microwave Conference*, 95–98, Bangkok, 2007.
11. Zhai, W.-S. and Y.-H. Zhang, "Apply Super-SVA to processing stepped frequency chirp signal with bandwidth gaps," *Journal of Electronics & Information Technology*, Vol. 31, No. 12, 2848–2852, 2009.
12. Zhai, W. and Y. Zhang, "Apply Super-SVA to SAR imaging with both aperture gaps and bandwidth gaps," *Proceedings of World Academy of Science, Engineering and Technology*, Vol. 57, 39–42, 2009.
13. Zhang, Y., J. Wu, and H. Li, "Two simple and efficient approaches for compressing stepped chirp signals," *AMPC 2005*, Vol. 2, 690–693, Suzhou, China, Dec. 4–7, 2005.
14. Zhang, Y., H. Li, and J. Wu, "Subaperture processing method for stepped frequency chirp signal," *System Engineering and Electronics*, Vol. 28, No. 1, 1–6, Jan. 2006.
15. Stankwitz, H. C., R. J. Dallaire, and J. R. Fienup, "Nonlinear apodization for sidelobe control in SAR imagery," *IEEE Trans. on Aerospace and Electronic Systems*, Vol. 31, No. 1, 267–279, 1995.